Coalescence of dry foam under water injection

Rémy Mensire, Keyvan Piroird, Elise Lorenceau

▶ To cite this version:

HAL Id: hal-01077425

https://hal-enpc.archives-ouvertes.fr/hal-01077425

Submitted on 24 Oct 2014

Collapse of a dry foam under water injection[†]

Rémy Mensire,[a] Keyvan Piroird,[a] and Elise Lorenceau,[*a]

When a small volume of pure water – typically a drop – is injected within an aqueous foam, it locally triggers the collapse of foam films, thus opening a cavity in the foam's bulk. We consider the final shape of this cavity and we quantify its volume as a function of the volume of injected water, the diameter of the bubbles and the liquid fraction of the foam and provide quantitative understanding to explain how and when this cavity appears. We epitomize the dilution of surfactants at the water-air interfaces as the main cause lying behind the breaking and coalescence process. Thus, this allows us to identify a new coalescence regime for which a critical surfactant concentration rules the stability of the films.

1 Introduction

Aqueous foams exhibit interesting physical features, such as high specific surface area, complex rheology, low specific gravity and large expansion ratio. These properties, which have been extensively studied from a fundamental point of view[1–3], explain why foams are used in a wide variety of technological applications such as enhanced oil recovery, detergency or fire-fighting technology. In the latter, light foams are spread on the surface of combustible solids or flammable fuels to extinguish an ongoing fire and to suppress re-ignition of the remaining liquid. Among the standardized fire tests that have been developed to assess the long term ability of foam to fight fire, the "deluge resistance time test" mimics the impact of pure water on foam, which may occur if the sprinkler system runs out of surfactants or if it rains heavily[3]. This test is critical to the long term stability of fire-fighting foams. Indeed, under persistent impacts of water drops, cavities may open in the foamy thermal insulating blanket that floats on the fuel surface, thus leading to fire re-ignition. The diameter of these cavities is often far larger than the mean diameter of the bubbles that constituted the foam, thus suggesting that the impact of water drops has induced catastrophic rupture of hundreds of bubbles. In this paper, we experimentally consider the volume of these cavities as a function of the volume of injected water, the diameter of the bubbles and the liquid fraction.

Our motivation is thus bound to the fundamental issue of the collective ruptures of foam films in aqueous foams. These ruptures can be triggered by water in the case of fire-fighting, or by any defoaming agents. In this context, water appears as a peculiar case. As it is fully miscible with the foaming solution, it can mix and propagate throughout the continuous phase of the aqueous phase. This dynamical process leads to a non-homogeneous distribution of surfactants at the water-air interfaces that induces rupture. In this experimental work, we thus discuss the rupture mechanism of foam induced by water injection and reveal a new critical criterion to explain the rupture avalanches with water.

2 Experiments

The foaming solution is a mixture composed of dodecanol at concentration 5.10^{-4} mol/L and TTAB (TetradecylTrimethylAmmoniumBromide) at concentration $C_i = 0.01$ mol/L, a value well above the CMC of 0.0033 mol/L. All the surfactants were purchased from Aldrich and used as received. The foaming solution has a surface tension at equilibrium $\gamma = 28 \pm 1$mN/m and the same viscosity and density as water ($\eta = 1$mPa.s and $\rho = 1000$ kg/m^3. To produce the foam, a slow flow of gaseous nitrogen is blown via a syringe needle into a rectangular column 27 cm-high and with a 6 cm-wide square base. Using two different syringe needles, we obtain foams with an average bubble diameter D_b either of 3.2 or 7.4 mm. The average bubble diameter is measured from analysis of images at the bottom of the foam column where the bubbles are spherical. This leads to uncertainty in the measurement of 20%

The mechanism leading to foam rupture under injection of pure water can be inferred from Figure 1a), showing the impact of a drop of water of radius 2 mm at 0.6 m/s on a dry aqueous foam XX.

Right after the impact, the drop passes through the foam films without breaking them and penetrate deep within the foam. Then, it vanishes and all the liquid is transferred to the foam. As the water from the drop flows into the foam, it induces the rupture of multiple foam films and leads to the

[a] Laboratoire Navier, UMR 8205 CNRS - ENPC ParisTech - IFSTTAR, Universit Paris-Est, 2 alle Kepler, 77420 Champs sur Marne; E-mail: elise.lorenceau@ifsttar.fr
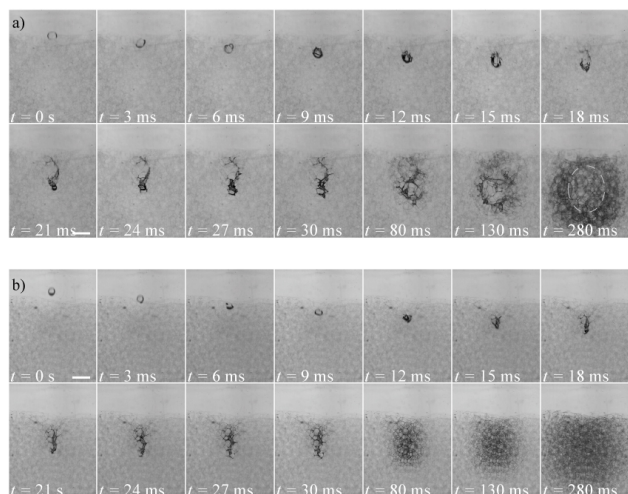
Fig. 1 Impacts of drops penetrating and falling into a dry aqueous foam with an initial velocity of 0.6 m/s. The scale bars correspond to 6 mm a) Impact of a drop of pure water. It quickly coalesces with the foam. The surfactant-free liquid is redistributed within the different elements of the liquid and spread homogeneously. Foam rupture is concomitant with this spreading and at $t =$280 ms an empty cavity - highlighted with a dotted white line - is left within the foam. b) Impact of a drop of foaming solution. It quickly coalesces with the liquid network of the foam. The liquid is redistributed within the different elements of the foam and spread homogeneously. No film rupture is observed.

opening of a cavity in the foam. We made the same experiment, but with a drop of the foaming solution that was used to generate the foam (Fig. 1b). In that case, the drop also penetrates a few millimetres into the foam and then starts flowing in the aqueous network. However, this time, none of the films break and the foam is not destroyed but simply wetter. In these experiments, the droplets and the foam bubbles have the same size, thus during the impact, each droplet hits different elements of the foam at the same time and it is rather unlikely to observe the impact on a single foam film. Yet, to qualitatively understand our observations, we recall features of the impact of a drop on an individual foam film[4–6]. Typically, slow droplets bounce off individual foam films, while quick droplets pass through without breaking the films. In addition to pure bouncing and crossing, these studies report partial coalescence events, where only some fraction of the impacting drop coalesces.

In our case, right after the impact, the two drops indeed pass through the first films without breaking them: after 10 ms, they are 5 mm deep in the foam, thus suggesting that the impacts with the surface of the foams have barely slowed them down. Yet, as each successive impact absorbs a small part of the original kinetic energy, the drops gradually decelerate down to a point where partial coalescence with the foam can

occur[4–6]. These successive coalescences leave a wet vertical wake behind the drops, and the foam locally appears darker due to a worse light transmission. These sudden additions of liquid are quickly distributed within the different elements of the foam liquid network, which are the foam films, the Plateau borders located at the junction of three films and the nodes or vertices located at the junction of four Plateau borders. Thus, wet fronts propagate within these different elements as predicted by foam drainage theory[3,7–12]. At $t = 280$ ms, they have nearly invaded the whole field of view of our camera. Yet, for the pure water drop, the front propagation is associated to a local dilution of surfactants. This lack of surface active agents induces the collapse of the foam films. Thus, at $t = 280$ ms, the impact of the water drop has generated an oblong empty cavity deep in the foam, while the impact of a foaming solution drop has left the foam intact.

To quantify the collapse due to the dilution of surfactants, we perform quiescent experiments, where a controlled volume of water is injected deep in the foam without initial velocity. In this paper, we study how the volume of the cavity depends on the injected volume of water, as well as on other parameters, such as the liquid fraction of the foam and the bubble size. Prior to any water injection, we wait for 20 minutes so that the foam reaches static equilibrium. This ensures a vertical gradient of liquid fraction in the foam due to a competition between capillarity and gravity: the foam at the top of the column is very dry while at the base of the column, the liquid fraction ε is close to 0.36, the random close packing fraction. This equilibrium being reached, a volume of water V, ranging between 4 and 10 μL, is injected at $t = 0$ within the 3D foam via a capillary tube of diameter 1.2 to 1.7 mm. Using a syringe pump, the injection of the whole volume is performed at constant injection rate of 14 mL/min. Thus, the capillary tube is emptied at most in 40 ms. We probe the resistance of foam under pure water at different injection heights H, where $H = 0$ corresponds to the base of the foam column. Typically, 7 cm $< H <$ 22 cm, which corresponds to foam at different initial liquid fraction ε_i. In this limit of very dry foam where the volume of liquid films is not negligible, we can not use recent results from literature[13]. Thus, to determine how ε_i varies with H, we proceed as follows: first, we write a balance between capillary and gravity that gives the variation of the pressure and of the radius of curvature of the slender Plateau borders as a function of height. Then, using the fits provided by Bergeron[14], we evaluate the thickness of the liquid films. The relation between ε_i and the injection height H is then calculated adding the volume of the different foam elements, including the films whose thickness is given as a function of the pressure[2]. This gives the results of Table I.

The foam is uniformly illuminated from one side, and the formation of the cavity is followed using a high-speed camera recording at 500 fps during 3 seconds as it can be seen in figure

| D_b \ H	7 cm	9 cm	14 cm	22 cm
3.2 mm	$6.1\ 10^{-4}$	$4.7\ 10^{-4}$	$3.2\ 10^{-4}$	$2.4\ 10^{-4}$
7.4 mm	$1.8\ 10^{-4}$	$1.5\ 10^{-4}$	$1.2\ 10^{-4}$	$0.9\ 10^{-4}$

Table 1 Liquid fraction values ε_i used in our experiments for different heights H and average bubble diameters D_b.
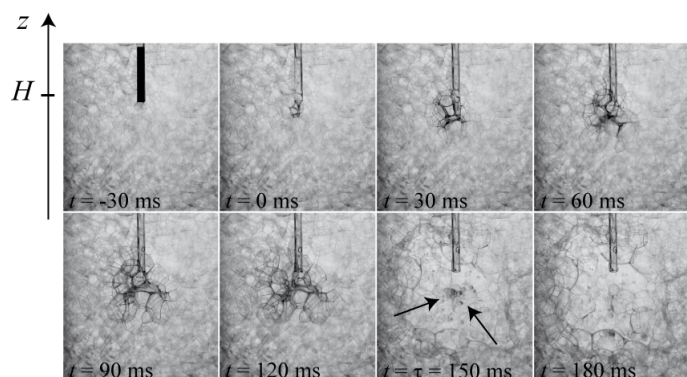
Fig. 2 Formation of a cavity in a dry foam with $D_b = 3.2$ mm. A water volume $V = 0.03$ mL - highlighted in the first image - is injected at constant velocity via a capillary tube of 1.7 mm diameter. The injection starts between the first and second image and terminates between the second and third image. The time interval between the images is 30 ms. The imbibition of the foam by water is followed with a violent explosion occurring at $t = \tau = 150$ ms, which leaves an empty spherical cavity of approximately 3 cm in the foam.

2 for a dry foam with $D_b = 3.2$ mm and $\varepsilon_i = 2.4.10^{-4}$.

The imbibition of the foam by water is followed by a sudden collapse of the foam at $t = \tau = 150$ ms after the end of water injection. This leaves a cavity in the foam of volume $\Omega \sim 10$ mL, thus suggesting a quasi-concomitant collapse of approximately 100 bubbles (see Fig 2 at $t = 150$ ms). We emphasize that at $t = \tau$, the foam beyond the limit of the cavity does not appear darker, suggesting that the liquid fraction of the foam beyond the limit of the cavity is still at ε_i. All the added liquid, which was comprised within the volume Ω before the rupture, is converted into tiny droplets highlighted with black arrows in Fig 2.

A digital camera records the light transmitted by the foam. We only consider foam constituted of big bubbles, which transmit light well. Moreover, the wetter and the thicker the foam, the darker it appears. Thus, the position of the edges of the cavity are characterized by a gradient in light transmission: the images are whiter where foam has collapsed while on the edge of the cavity, we observe a darker front due to the redistribution of liquid[15]. We therefore track gradient in light transmission of our images using imageJ software and obtain
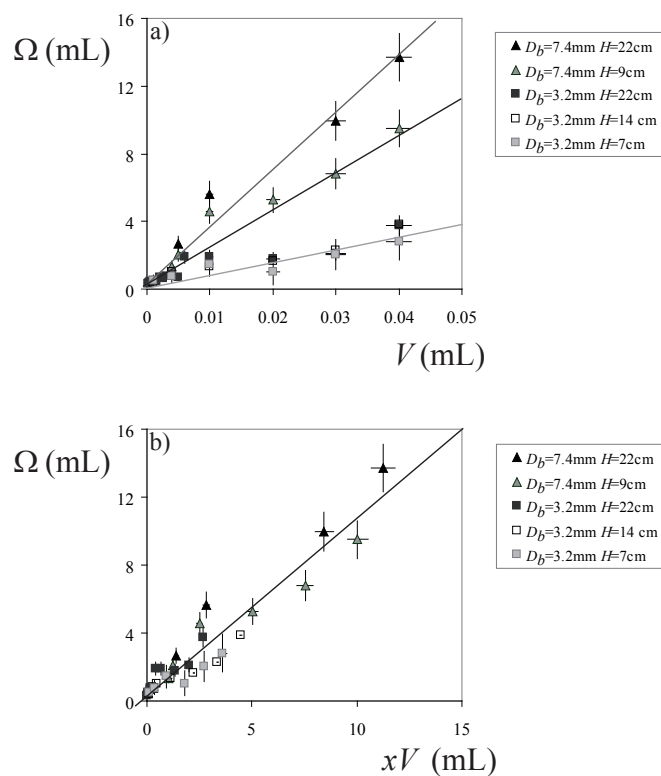
Fig. 3 For two bubble diameters $D_b = 3.2$ and 7.4 mm and three different injection heights $H = 7$, 9, 14 and 22 cm. a) Cavity volume Ω as a function of the injected volume of water V. The different lines are here to guide the eyes. b) The same data as a function of the rescaled injected volume xV. The line is a fit of equation $Y = X$.

oblate surfaces characteristic of the cavity volume. These surfaces are fit by an ellipse with a vertical semi-axis b and a horizontal semi-axis a. We always observe that $b > a$: this is due to gravity which induces a non-isotropic diffusion of water in the foam in the z direction. However, in the horizontal plane, the imbibition is isotropic. We thus deduce the volume of the cavity from the volume of the ellipsoid of revolution with a vertical axis of symmetry and with a pair of equal semi-axes a and a distinct third semi-axis b, which reads $\Omega = \frac{4}{3}\pi ab^2$. The error margin on a and b is of the order of 1 mm, which gives a relative error of 30 % for the smallest volumes of cavity (typically less than 4 mL) and less than 10 % for the highest volumes. In figure 4a, we report the volume Ω as a function of the injected volume V of water. Ω increases with V, D_b and H. This suggests that when the dilution is important, the foam dry and the bubbles big, the cavities get larger.
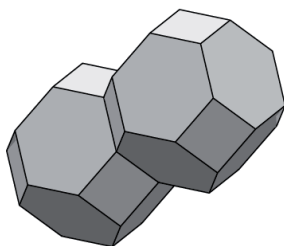
Fig. 4 Two elementary foam cells constituted of two truncated octahedrons. Each thick line corresponds to a Plateau border. Figure obtained using the software surface evolver[24].

3 Discussion

To understand these observations, we recall different features concerning coalescence of dry foams or emulsions. Catastrophic foam coalescences have been observed in 3D draining foams[16]. Those cascade events are mainly localized where the liquid fraction is the lowest hence at the top of the draining column[17,18]. This localization suggests that almost all of the coalescence events occur where the foam is the dryer, hence for liquid fraction below a critical value ε_f as proposed by Carrier and Colin[19]. Recent experiments in foams or emulsions link those catastrophic coalescence to dynamical events[20,21]. In foams, those dynamical rearrangements, known as T1, involve the disappearance of a thin film followed by the creation of a thick foam film in a different direction. Therefore, if $\varepsilon < \varepsilon_f$, the amount of liquid that is locally available is insufficient to draw the new thick film. This triggers another aborted bubble rearrangement, leading to a catastrophic process[20]. Stability criteria have also been drawn for emulsions over a wide range of concentration[22] and can be characterized by two macroscopic parameters: a minimum value of surfactant concentration and a maximum value of osmotic pressure, which corresponds to the pressure exerted upon the interfaces. As the osmotic pressure in disordered emulsions only depends on liquid fraction[13,23], these features concerning emulsions can be understood using the framework proposed by Carrier and Colin for aqueous foams[19]. Coalescence in both foams and emulsions is governed by critical values of local liquid fraction ε_f and surfactant concentration C_f. ε_f does not depend on the size of the bubbles but rather on the chemical composition of the surfactants[19,20] and, as already mentionned, of their concentration.

Only few works strive to determine how ε_f and C_f are linked. Two limiting cases can be drawn: for a surfactant-free solution, foam films are truly unstable, thus suggesting that $\varepsilon_f = 1$. In the opposite limit of infinitely stable foam, $\varepsilon_f = 0$. In the range of surfactant concentration typically used in foaming solution CMC$< C_i <$ 100 CMC, ε_f barely varies

with C_i as can be observed in figure 5 where some of the data of reference[19] has been reported. For TTAB, ε_f is constant for $C_i >>$CMC and slightly decreases around the CMC[19]. There is no data concerning the coalescence of foams below the CMC, but the critical osmotic pressure of emulsions, hence the critical liquid fraction of emulsions has been shown to quickly diverges up to 1 when the surfactant concentration reaches a critical concentration value of one third of the CMC[22]. Thus, below this value, emulsions are unstable.

To understand what determines the size of the foam cavity Ω, we evaluate both C_f, the local surfactant concentration and ε_f, the liquid fraction at $z = H$ just before the coalescence. Indeed, in our experiments, those two quantities simultaneously vary. The injection of pure water through the foam decreases the local concentration in surfactants from C_i to C_f and increases the local liquid fraction from its initial value ε_i up to the critical value ε_f for which the foam ruptures.

As the imbibition dynamics is slower than the rupture dynamics, the liquid fraction of rupture ε_f can be evaluated from volume conservation within Ω. Indeed, the liquid fraction of rupture is the initial liquid fraction to which the volume of fresh liquid V that is comprised within Ω is added. Therefore, $\varepsilon_f = \varepsilon_i + V/\Omega$.

When introduced into an aqueous solution, surfactants distribute to the interface and to the bulk. Thus, the number of surfactants n in Ω writes $n = C\varepsilon\Omega + 2\Gamma\Sigma$, where ε is the liquid fraction, C is the bulk concentration of surfactants, Σ is the area of the air/water interface and Γ the surface excess of surfactants at the air/water interface. Assuming a rapid dilution of the surfactant due to water injection and homogenous bulk and surface concentrations of surfactants at $t = \tau^-$, we write the conservation of surfactants n between $t = 0$ and $t = \tau^-$. Using the subscript f for the different parameter at $t = \tau^-$ yields :

$$n = C_i\varepsilon_i\Omega + 2\Gamma_i\Sigma_i = C_f\varepsilon_f\Omega + 2\Gamma_f\Sigma_f \qquad (1)$$

For $t < \tau$, we do not observe any coalescence (see figure 2), hence $\Sigma_i = \Sigma_f$. Moreover, Σ_i is linked to the volume of the cavity Ω and the diameter of the bubble D_b and can be calculated assuming an ideal structure for the foam such as the one provided by the Kelvin structure depicted in Figure XX. Each individual cell of this structure has 8 hexagonal faces, 6 square faces and 36 edges, each of length l. The total surface area S_K of a Kelvin cell is $S_K = (12\sqrt{3}+6)l^2$ while its volume is $V_K = 8\sqrt{2}l^3$. Introducing the bubble diameter also provides $V_k = (\pi/6)D_b^3$, hence $D_b = 2.78l^2$. In the cavity of volume Ω, the number of bubbles N_b is $N_b \sim \Omega/\left((\pi/6)D_b^3\right)$, which finally yields $\Sigma = N_b S_K = 6.58\Omega/D_b$.

Below the CMC, the surface excess of ionic surfactant molecules Γ is given by the Gibbs equation[25], where the factor 2 in the denominator appears because of the activity of the

electrolyte Na^+ :

$$\Gamma = -\frac{1}{2RT}\left(\frac{\partial \gamma}{\partial \ln C}\right)_{T,P} \qquad (2)$$

As proposed by Simister *et al.*,[26], Γ can be determined from a quadratic fit of the plot of the surface tension γ against $\ln C$ such as $\gamma = \alpha(\ln C)^2 + \beta \ln C + \delta$. This gives a logarithmic variation of Γ as a function of C such as $\Gamma(C) = 2\alpha \ln C + \beta$. This relation has been verified for TTAB solutions measuring the surface excess Γ with neutron reflection[27]. In our case, it gives $\alpha = -2.6 10^{-3}$ mol/m^2 and $\beta = -48.3 10^{-3}$ mol/m^2.

If n is indeed constant between $t = 0$ and $t = \tau^-$, these remarks and equation 1 suggest a linear relation between Ω and V such as :

$$\Omega = xV = \frac{C_f}{\varepsilon_i\left(C_i - C_f\right) + 13.2\frac{\Gamma_i - \Gamma_f}{D_b}}V \qquad (3)$$

The numerical coefficients of equation 3 being explicitly calculated, we adjust C_f to obtain a slope of 1 between Ω and xV for $D_b = 3.2$ and 7.4 mm. This allows us to obtain indirect measurements of C_f as a function of D_b for three different initial liquid fraction ε_i (or injection heights), which yields $C_f(D_b = 3.2$ mm$) = (0.8 \pm 0.2).10^{-3}$ mol/L and $C_f(D_b = 7.4$ mm$) = (1.2 \pm 0.3).10^{-3}$ mol/L. The validity of this approach is confirmed in figure 4b), where a reasonable collapse of the data on the line $\Omega = xV$ is observed for the different injection heights.

The two critical values of C_f are very close, thus suggesting that C_f barely depends on the bubble diameter. Moreover, they are both lower than the CMC, which is equal to $3.3.10^{-3}$ mol/L. This is in agreement with observations concerning emulsions[22], in which a critical surfactant concentration of one-third the CMC, independent of the drops' radius has been reported. We also evaluate the mean liquid fraction of rupture $\langle \varepsilon_f \rangle$ for the two bubble diameters by averaging the relation $\varepsilon_f = \varepsilon_i + V/\Omega$ on all data points. These results are compared with those provided by Carrier and Colin for the critical liquid fraction of foam coalescence for TTAB solution at various concentrations (see Figure 5).

Above the CMC, the critical liquid fraction $\langle \varepsilon_f \rangle$ is nearly constant $\langle \varepsilon_f \rangle \sim 5.10^{-4}$, independent of the bubble radius and of the surfactant concentration, while below the CMC, the critical liquid fraction increases quickly up to values between 3.10^{-3} to 7.10^{-3}. The large uncertainty of the critical value of liquid fraction below the CMC also reflects this divergence. The results in figure 5 therefore suggests two different regimes for foam collapse depending on surfactant concentrations. As previously mentioned, if $\varepsilon < \varepsilon_f$ and $C_i >$CMC, foam coalescence is triggered by topological rearrangements, which are randomly distributed in the section of the foam. This mechanism explains that i) the collapse occurs where the foam is
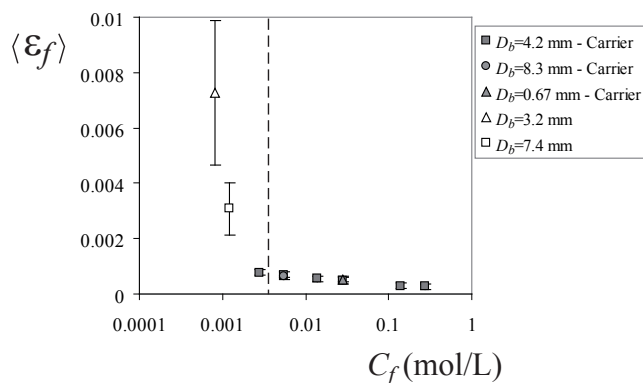
Fig. 5 Mean critical liquid fraction $\langle \varepsilon_f \rangle$ for foam rupture as a function of the critical concentration in surfactants C_f, Adapted with permission from Carrier and Colin, Langmuir, 19, 4535, 2003. Copyright 2003 American Chemical Society. The grey points correspond to Carrier and Colin data for various bubble radius [19] while the open points correspond to this paper data. The dashed line shows the CMC. Above the CMC, the critical liquid fraction $\langle \varepsilon_f \rangle$ is nearly constant $\varepsilon_f \sim 5.10^{-4}$, independent of the bubble radius and of the surfactant concentration, while below the CMC, the critical liquid fraction is much higher ranging between 3.10^{-3} to 7.10^{-3}.

the driest, hence at the top of the foam ii) the dynamics of the collapsing foam is discontinuous and evolves by sudden bursts of activity[3,17,18]. However, when the surfactant concentration reaches value smaller than the CMC, collapse occurs quickly after the end of the water injection. In this regime, the collapse is characterized by a critical value of surfactant concentration C_f rather than by a critical value of liquid fraction. The local mechanisms of coalescence likely involves dilution of the foaming solution by pure water and induces inhomogeneity in surface tension between Plateau borders and foam films. This may create Marangoni flows and enhanced capillary suction from the foam films to the Plateau borders that may result in rapid thinning and break-up of the fragile foam films.

4   Conclusion

By injecting a given volume of pure water through a dry aqueous foam, we probe its stability under coalescence. Assuming a rapid equilibrium of the surfactants under dilution, we quantify a new regime of simultaneous coalescence characterized by a critical value of the concentration of surfactant. This poor-surfactant coalescence regime is very different from the rich-surfactant coalescence regime highlighted in[3,19], characterized by a critical value of another macroscopic parameter that is the liquid fraction of the foam. In this regime, a local break up propagative mechanism, involving dynamical rearrangement of bubbles, has been characterized[20]. Beyond these fundamental aspects, our work also helps answering practical questions associated to the stability of fire fighting aqueous

foams under pouring rain.

There is still a need for understanding the local break-up mechanism in this surfactant-poor regime. However, this microscopic understanding, which might involve rapid thinning of foam films induced by Marangoni flows due to inhomogeneity of surface tension, is beyond the scope of this work.

Acknowledgements

References

1 D. Weaire and S. Hutzler, *The Physics of Foams*, Oxford University Press, 1999.

2 I. Cantat, S. Cohen-Addad, F. Elias, F. Graner, R. Höhler, O. Pitois, F. Rouyer and A. Saint-Jalmes, *Foams : Structure and Dynamics*, Oxford University Press, 2013.

3 P. Stevenson, *Foam Engineering - Fundamental and Applications*, Wiley-Blackwell, 2012.

4 L. Courbin and H. A. Stone, *Phys. Fluids*, 2006, **18**, 091105.

5 A. Le Goff, L. Courbin, H. A. Stone and D. Quere, *EPL*, 2008, **84**, 36001.

6 T. Gilet and J. W. Bush, *J. Fluid Mech.*, 2009, **625**, 167–203.

7 R. Leonard and R. Lemlich, *AICHE J.*, 1965, **11**, 18–24.

8 G. Verbist and D. Weaire, *Europhys. Lett.*, 1994, **26**, 631–634.

9 S. Koehler, H. Stone, M. Brenner and J. Eggers, *Phys. Rev. E*, 1998, **58**, 2097–2106.

10 S. Koehler, S. Hilgenfeldt and H. Stone, *Langmuir*, 2000, **16**, 6327–6341.

11 M. Durand, G. Martinoty and D. Langevin, *Phys. Rev. E*, 1999, **60**, R6307–R6308.

12 S. Cohen-Addad, R. Hohler and O. Pitois, *Ann. Rev. Fluid Mech.*, 2013, **45**, 241–267.

13 A. Maestro, W. Drenckhan, E. Rio and R. Hoehler, *Soft Matter*, 2013, **9**, 2531–2540.

14 V. Bergeron, *Langmuir*, 1997, **13**, 3474–3482.

15 M. Vera, A. Saint-Jalmes and D. Durian, *Appl. Opt.*, 2001, **40**, 4210–4214.

16 W. Muller and J. di Meglio, *J. Phys. Cond. Matt.*, 1999, **11**, L209–L215.

17 N. Vandewalle, J. Lentz, S. Dorbolo and F. Brisbois, *Phys. Rev. Lett.*, 2001, **86**, 179–182.

18 N. Vandewalle and J. Lentz, *Phys. Rev. E*, 2001, **64**, 021507.

19 V. Carrier and A. Colin, *Langmuir*, 2003, **19**, 4535–4538.

20 A.-L. Biance, A. Delbos and O. Pitois, *Phys. Rev. Lett.*, 2011, **106**, 068301.

21 N. Bremond, H. Domejean and J. Bibette, *Phys. Rev. Lett.*, 2011, **106**, 214502.

22 J. Bibette, D. Morse, T. Witten and D. Weitz, *Phys. Rev. Lett.*, 1992, **69**, 2439–2442.

23 R. Hohler, Y. Yip Cheung Sang, E. Lorenceau and S. Cohen-Addad, *Langmuir*, 2008, **24**, 418–425.

24 B. K., *Exp. Math.*, 1992, **1**, 141–165.

25 G. A. Adamson A. W., *Physical Chemistry of surfaces*, Wiley-Interscience, 2012.

26 E. Simister, R. Thomas, J. Penfold, R. Aveyard, B. Binks, P. Cooper, P. Fletcher, J. Lu and A. Sokolowski, *J. Phys. Chem.*, 1992, **96**, 1383–1388.

27 J. Lu, R. Thomas and J. Penfold, *Adv. Coll. Int. Sci.*, 2000, **84**, 143–304.